Absolute rate coefficients for the recombination of open f-shell tungsten ions

2014 J. Phys.: Conf. Ser. 488 012051

(http://iopscience.iop.org/1742-6596/488/1/012051)

XXVIII International Conference on Photonic, Electronic and Atomic Collisions (ICPEAC 2013) IOP Publishing
Journal of Physics: Conference Series **488** (2014) 012051 doi:10.1088/1742-6596/488/1/012051

Absolute rate coefficients for the recombination of open f-shell tungsten ions

C Krantz[1], K Spruck[2], N R Badnell[3], A Becker[1], D Bernhardt[2], M Grieser[1], M Hahn[4], O Novotný[4], R Repnow[1], D W Savin[4], A Wolf[1], A Müller[2] and S Schippers[2]

[1] Max-Planck-Institut für Kernphysik, 69117 Heidelberg, Germany
[2] Institut für Atom- und Molekülphysik, Justus-Liebig-Universität Gießen, 35392 Gießen, Germany
[3] Department of Physics, University of Strathclyde, Glasgow G4 0NG, United Kingdom
[4] Columbia Astrophysics Laboratory, Columbia University, New York, NY 10027, USA

E-mail: claude.krantz@mpi-hd.mpg.de

Abstract. We have carried out direct measurements of the absolute recombination rate coefficients of four charge states of tungsten in the range from W^{18+} to W^{21+} in a heavy ion storage ring. We find that the rich atomic fine structure of the open f-shell leads to very high resonant enhancement of the recombination rate at energies below ∼50 eV. Even in the higher energy domain relevant to fusion plasma this leads to a recombination rate coefficient that is more than four times higher than predicted by the commonly used ADAS database of recombination rates. In addition to the experimental measurements we have carried out theoretical calculations using AUTOSTRUCTURE. For W^{20+} these predict a plasma recombination rate coefficient that agrees much better with the measurement than the ADAS model but still fail to reproduce the experimental data in detail.

1. Introduction

Spectroscopy and electron collision reactions of highly charged tungsten have received much attention in the fusion plasma community. Tungsten has been established as the coating material of choice for strongly exposed plasma facing surfaces in tokamak-type plasma devices for its ability to withstand extreme thermal loads [1, 2, 3]. In fact, most of the high-energy tokamak experiments in operation (JET, ASDEX-Upgrade, JT60-U) or under construction (ITER) are designed to use tungsten as surface material for their divertor sections which are exposed to a particularly intense particle bombardment of products and contaminants extracted from the stored plasma cloud [3, 4].

A resulting contamination of the plasma by tungsten atoms sputtered off the irradiated walls cannot be avoided completely. As they migrate towards the inner and hotter regions of the tokamak plasma, the tungsten atoms are collisionally ionized by electron impact up to equilibrium with electron recombination at the local plasma temperature. At JET, ionization stages near W^{20+} are observed next to the separatrix of the stored plasma, while much higher charge states (around W^{44+}) dominate in the core plasma. Recombination with free electrons leads to emission of photons and thereby energy loss from the plasma. Due to the depth of their Coulomb potential wells, the highly charged tungsten ions emit fairly energetic radiation at

every recombination event and, hence, are rather efficient cooling agents. Thus, their population density must be kept low in nuclear fusion reactors in order to maintain high plasma temperatures [5].

At ASDEX-Upgrade, where all plasma facing chamber walls have been tungsten plated [2], extensive in-situ measurements of the VUV to X-ray emission from highly charged tungsten contaminants in the plasma have been carried out. As the observation column of the spectrometer necessarily crosses regions of different temperature of the toroidal plasma, many different tungsten charge states contribute to any given measured emission spectrum [6]. Knowledge of the temperature dependent recombination and ionization rate coefficients is therefore required in order to disentangle the data. However, detailed theoretical studies on the atomic structure of partially ionized high Z elements are rare. This is especially true for electron recombination, which – in the energy domain relevant to fusion plasmas – proceeds almost exclusively via resonant processes like dielectronic recombination (DR) and is difficult to model reliably without thorough atomic structure calculations. The latter can be numerically quite demanding in cases where many valence electrons participate in the recombination process, e.g., for charge states with open d or f shells. Hence, until recently, detailed quantum mechanical calculations had been performed on only a few very highly ionized charge states of tungsten [7, 8, 9, 10].

In an analysis of soft X-ray to VUV spectra measured at ASDEX-Upgrade, Pütterich et al. have used the generic recombination rates from the ADAS data base, but found that empirical correction factors ranging from 0.3 to 2.2 were necessary in order to bring the predicted charge state abundances into agreement with the measurements [6]. It appeared that most recombination rates in the range of charge states W^{20+} to W^{55+} were predicted too low when using the recombination rates from the ADAS data set.

In an effort to provide a sound experimental basis for calculations of the recombination rate coefficients of open f-shell tungsten ions, we have conducted a series of measurements at the heavy ion storage ring TSR of the Max Planck Institute for Nuclear Physics (MPIK) in Heidelberg, Germany. TSR is an electron cooler storage ring fed by a 12 MV Tandem Van-de-Graff accelerator, and thereby ideally suited for systematic studies of electron-ion collision reactions of a wide range of highly charged atomic ion species. So far, we have measured detailed energy resolved recombination rate coefficients for $W^{18+}(4f^{10})$, $W^{19+}(4f^{9})$, $W^{20+}(4f^{8})$, and $W^{21+}(4f^{7})$. In addition, we have performed theoretical calculations of recombination rate coefficients for these ions employing the AUTOSTRUCTURE code.

2. Experiment

An electron-ion recombination experiment in a heavy-ion storage ring has several fundamental advantages over other approaches. A storage ring acts as a very fine momentum selector, i.e., ions can be stored with a well defined mass and charge state, as opposed to devices storing high-temperature plasma clouds where a multitude of different ionization stages are present that need to be disentangled by data analysis. Storage also allows the ions to de-excite to the ground state so that recombination experiments can be performed on a well known initial state population, which makes comparison to theoretical models straight forward. Electron cooling in the storage ring reduces the kinetic temperature of the initially hot ions by multiple Coulomb scattering within a cold, velocity matched electron beam [11], resulting in a velocity spread of the stored ions that is much narrower than that of the cooler electrons. In subsequent collision experiments – performed by detuning the average velocity of the cooler electrons with respect to the stored ions – the energy resolution is thus mainly defined by the temperature of the electron beam and can be as good as a few meV for small collision velocities [12].

Highly charged tungsten ions in the range from W^{18+} to W^{21+} were produced at the heavy ion beam facility of the MPIK by acceleration and foil induced electron stripping in a 12 MV Tandem

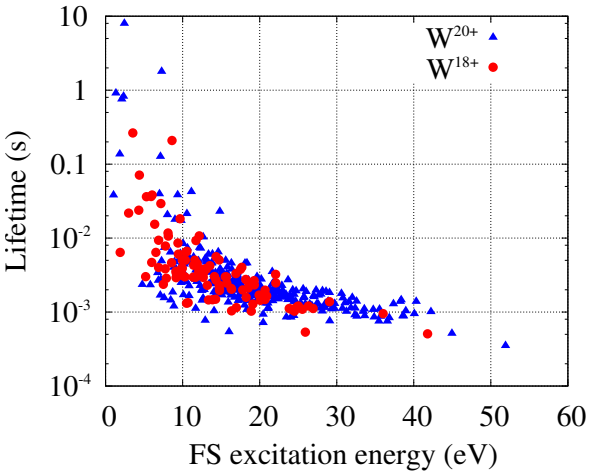

Figure 1. (Color online) Calculated fine structure (FS) levels above the ground states of $W^{20+}(4d^{10}\,4f^{8}\ {}^{7}F_{6}$, blue triangles) and $W^{18+}(4d^{10}\,4f^{10}\ {}^{5}I_{8}$, red dots) and associated lifetimes. For each ion, a single state with very long lifetime (7×10^{4} s and 5×10^{8} s) is off scale.

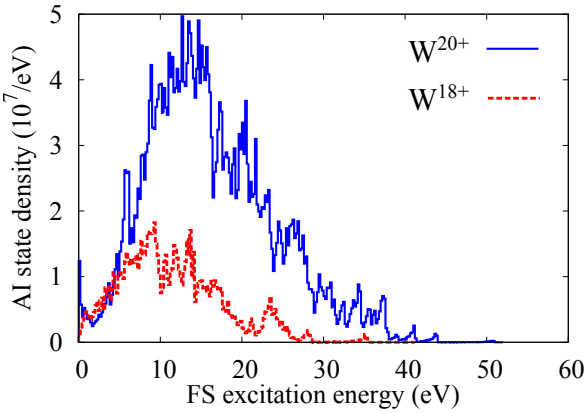

Figure 2. (Color online) Density of autoionizing states contributing to dielectronic recombination by fine-structure excitation of the ground states of W^{20+} (solid blue histogram) and W^{18+} (dashed red), calculated using the levels from Fig. 1 and a hydrogenic approximation of the binding energies of the Rydberg electron.

Van-de-Graff accelerator. Negatively charged tungsten carbide, obtained from a Cs sputter source, was used as a precursor species. After acceleration and charge state selection the ion beams were injected into the TSR storage ring at kinetic energies ranging from 166 MeV (W^{18+}) to 208 MeV (W^{21+}). In principle, multiturn injection and electron cooler assisted injection stacking [13] allow to store quite high ion currents in the TSR. However, for the tungsten charge states discussed in this work, a very low production efficiency in combination with short ion beam lifetimes in the ring ($\sim$ few s) led to unmeasurably low stored ion currents, estimated to be on the order of a few nA [14]. This is well below the sensitivity limit of the TSR's built-in current diagnostics.

Measurements started a few seconds after beam injection in order to allow the ion cloud to cool down via interactions with the electron cooler, and in order to allow excited atomic states produced during the foil-stripping process to relax. Figure 1 displays the calculated lifetimes of all fine structure levels associated with the ground state configurations of $W^{18+}(4d^{10}\,4f^{10})$ and $W^{20+}(4d^{10}\,4f^{8})$, respectively. The level energies were obtained using the atomic structure code of Cowan [15]. Fine structure level lifetimes were computed taking into account all possible $E2$ and $M1$ transitions to lower levels from any given excited level. The large majority of lifetimes are well below 1 s, but the calculation does yield some levels that could remain populated even after several seconds of storage in the TSR, these being $W^{20+}({}^{3}O_{12};\ {}^{7}F_{0};\ {}^{5}L_{8})$ and $W^{18+}({}^{5}S_{2})$. Resonant recombination starting from an excited state is diminished by autoionization into lower lying states of the parent ion, hence a large metastable population in the ion beam could lead to underestimation of the recombination rate coefficient from the ground state. The experiment provides no hint about the amount of metastables left a few seconds after beam injection in the TSR. However, comparison with theory suggests that their impact on the measured overall rate coefficient was insignificant within the experimental uncertainty, as will be discussed below [16].

After electron cooling, the cooler electron beam was detuned from the ion velocity such that the desired collision energy among electrons and ions occurred. In this way, a collision energy range from 0 eV to several 100 eV was scanned for each ion. Recombination products leave the closed orbit of the stored beam at the next bending magnet of the TSR following the electron

cooler section. Due to their high energy and low emittance, the products can be collected on a small-scale single particle counting detector with an efficiency of practically 100% [17]. The energy-resolved experimental recombination rate coefficient relates to the measured product count rate R by

$$\alpha(E) = \frac{R}{N_\mathrm{i} n_\mathrm{e} \eta} \frac{C}{L} \left(\frac{1}{1 - \beta_\mathrm{i} \beta_\mathrm{e}} \right) , \tag{1}$$

where $\eta \approx 1$ is the detector efficiency, C/L is the ratio between the circumference of the closed orbit in the TSR and the effective electron cooler length, β_i and β_e are the ion and electron velocities, respectively, in units of the speed of light, n_e is the cooler electron density, and N_i is the number of ions stored in the ring.

N_i is usually derived from a direct measurement of the stored ion current. However, as mentioned above, in the case of highly charged tungsten the ion beams were too faint to be measured by the TSR current diagnostics. Instead, a second counting detector was used to record the production rate of ionization products in addition to recombination. In all four tungsten experiments, the electron collision energy was kept well below the single ionization threshold. Hence, ionized products could originate only from collisions of the tungsten ions with residual gas molecules in the TSR beam pipe. The ionization rate could thus serve as a proxy signal for the ion current if one neglected possible variations in the vacuum pressure during the experiments.

Using the ionization rate as a proxy for N_i, a *relative* recombination rate coefficient could be derived from the measured data using eq. (1). In order to put the result on an absolute scale, the recombination rate coefficient at a single collision energy had to be measured independently. This was done by switching the cooler electron beam on and off and by comparing the corresponding ion beam lifetimes, τ_on and τ_off, in the TSR under both conditions. With the electron cooler switched off, the ion lifetime is defined by the probability of residual gas collisions. With the electron beam present, electron recombination drains the ion population as well (and can shorten the beam lifetime considerably at high electron density). The *absolute* recombination rate coefficient at a certain electron collision energy can then be derived from the difference of the inverse beam lifetimes. It is convenient to do this measurement with velocity-matched beams, i.e., at $E = 0\,\mathrm{eV}$, so that the mean ion velocity stays constant during interaction with the electron beam. The absolute recombination rate coefficient at 0 eV is then

$$\alpha(0\,\mathrm{eV}) = \frac{\tau_\mathrm{on}^{-1} - \tau_\mathrm{off}^{-1}}{n_\mathrm{e}} \frac{C}{L} , \tag{2}$$

as has been shown elsewhere [18, 19]. Overall, the experimentally derived recombination rate coefficient can be estimated to be accurate within 20% [14].

3. Results

While fast recombination has been observed previously for ions with complex valence shells [20, 21, 22], to the best of our knowledge, the recombination rate coefficients we found for W^{18+} to W^{21+} are among the highest ever measured [14, 23, 24]. As shown in Fig. 3, the recombination rate coefficient of W^{20+} exhibits very strong enhancement compared to the calculated rate coefficient for radiative recombination (RR) up to collision energies of at least 100 eV. Near 0 eV, a recombination rate coefficient of $\sim 10^{-6}\,\mathrm{cm^3 s^{-1}}$ is observed, i.e., three orders of magnitude higher than the calculated RR. For the other charge states, similarly high rate coefficients are found [23]. The resonant features visible in the data suggest that the rate enhancement is caused by a dense unresolved spectrum of autoionizing states contributing to the recombination. No individual lines are observed, the visible structures are much broader than the experimental energy spread.

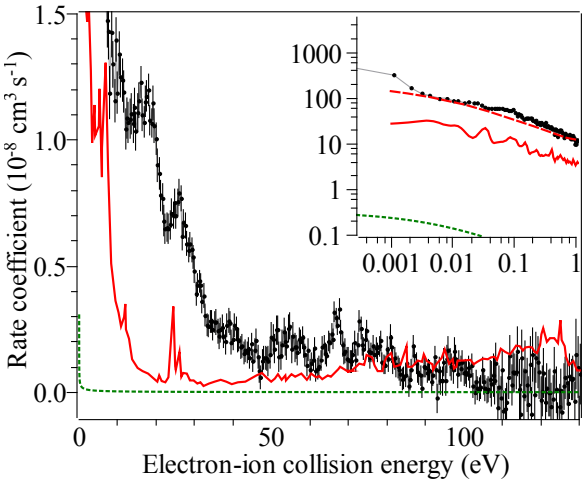

Figure 3. (Color online) Measured recombination rate coefficient for W^{20+}. The inset displays the data below an electron-ion collision energy of 1 eV on logarithmic scales. The short-dashed green curve shows the recombination rate coefficient expected for a purely radiative recombination involving no resonant processes [14]. Also shown are theoretical results by Badnell et al. [16] for intermediate coupling (IC) calculations (full red line) and fully partitioned low-energy estimate (long-dashed red line in the inset).

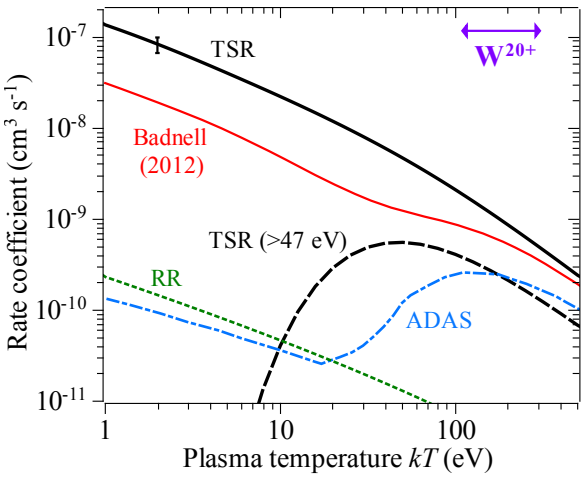

Figure 4. (Color online) Experimental plasma recombination rate coefficient for W^{20+} derived from the energy resolved data of Fig. 3 (thick black curve) [14]. Also shown are the theoretical rate coefficients for purely radiative recombination (short dashed green), the recommended values from the ADAS database (dash-dotted blue), and the new IC calculation by Badnell et al. (solid red) [16]. The double arrow indicates the plasma temperature region where the abundance of W^{20+} is greater than 1% [6].

Comparison with Fig. 1 reveals that the steep increase in the measured recombination rate coefficient of W^{20+} below 47 eV matches the energy range of the calculated spectrum of $4f^8$ fine structure excitations. In that energy interval, 292 excited levels of W^{20+} are predicted by the atomic structure code of Cowan [15]. Even a naive calculation, taking into account strictly dielectronic recombination only, reveals that the spectrum of autoionizing states associated with those fine structure excitations must be extremely dense. Using a simple hydrogenic approximation for the binding energies of the captured Rydberg electron and taking into account that Rydberg states beyond $n = 72$ cannot contribute to recombination as they are field-ionized in the bending magnets of the storage ring, one derives a total of approximately 7×10^8 DR resonant states in the continuum of W^{20+} below 47 eV [14]. For the 105 fine structure core excitations of W^{18+} a similarly high number of 2×10^8 autoionizing states below 30 eV is expected. The corresponding density of DR states at low collision energy hence lies in the order of 10^7 eV^{-1} in both cases (cf. Fig. 2).

In a theoretical work triggered by the experimental findings, Badnell et al. have carried out detailed atomic structure calculations on recombination of W^{20+} using the AUTOSTRUCTURE code [16]. In contrast to the naive picture of single fine structure DR resonances described above, their intermediate coupling (IC) code allows for configuration mixing of autoionizing levels consisting of one or several valence electron promotions and a single captured Rydberg electron. The resulting theoretical recombination rate coefficient is depicted in Fig. 3 (solid red curve). While the calculation does reproduce the overall shape of the measured data, the experimental rate coefficient is still higher by a factor of ~ 3 at low collision energies. Badnell

et al. attribute this to incomplete state mixing in their IC model as, for practical reasons, only a limited number of states can be allowed in the computation. For energies below 1 eV, theory can match the experiment when assuming full mixing of all states in this energy region [16]. In Fig. 3 (dashed red curve in the inset) the result of this ad hoc estimate is referred to as the fully partitioned, low energy estimate. Using the same approach of chaotic mixing of many multi-excited recombination resonances, Dzuba et al. achieve a similar degree of agreement with experiment in this energy regime [25].

The fully partitioned calculation mixes all multiply excited autoionizing levels within a relatively broad energy range around the singly-excited doorway level that is populated at given collision energy of the captured electron. The autoionization rate of the doorway level is thereby redistributed over a large number of mixing levels and the overall probability of radiative stabilization reaches almost unity [26]. Fully partitioned theory is believed to give a good estimate of the true recombination rate coefficient that would be reached by the IC calculation in absence of computational limitations. Moreover, the calculations assume that all recombination proceeds via excitation from the $^7F_6$ ground level of W^{20+}. The fact that they agree quite well with the measurement hence suggests that the possible metastable population of the W^{20+} ion beam, as discussed in the previous section, was small. Our measured plasma rate coefficient can therefore be assumed to be valid for recombination from the W^{20+} ground state within the experimental uncertainty of $\pm 20\%$.

At temperatures below $10\,\mathrm{eV}/k_\mathrm{B}$, our experimental plasma rate coefficient for W^{20+}, derived by convolution of the energy resolved data set from Fig. 3, is three orders of magnitude higher than the recommended value from the ADAS database (cf. Fig. 4). Although the abundance of W^{20+} peaks at considerably higher plasma temperatures around $160\,\mathrm{eV}/k_\mathrm{B}$, the enormous resonant enhancement of the recombination rate coefficient at low collision energies dominates the plasma recombination rate coefficient of the ion even in the temperature domain relevant to tokamak plasmas, where the measured rate coefficient still exceeds the ADAS values by more than a factor of four. An artificial data set obtained by removing all resonant structures below 47 eV from the experimental rate coefficient measured for W^{20+} (thick dashed black curve in Fig. 4) results in much better agreement with the ADAS plasma rate coefficient. This suggests that the discrepancy is largely due to neglected resonant recombination associated with fine-structure excitation of the ionic core. The recent IC theory by Badnell et al. [16] is in much better agreement with the measured rate coefficient, while still falling behind the experiment by up to a factor of four at low plasma temperatures.

4. Conclusion

We have measured absolute recombination rate coefficients of a series of highly charged tungsten ions in the charge state range from W^{18+} to W^{21+}. We have found extremely high recombination rates at electron-ion collision energies below $\sim 50\,\mathrm{eV}$. Similarly high rate coefficients were found for the remaining measured charge states, the analysis of which is ongoing [23]. We attribute these effects to a dense spectrum of recombination resonances related to fine-structure excitations of the ionic core. In the case of W^{20+} this interpretation is backed by an updated atomic structure calculation of the recombination process which predicts rate coefficient enhancement due to mixing of multi-excited states in the continuum of the parent ion [16]. Our results are of interest to the fusion plasma community, as the previously disregarded low energy resonant recombination of open f-shell tungsten ions boosts the plasma recombination rate significantly with respect to the recommended values from the ADAS data base, even in the much higher plasma temperature regime relevant to tokamak devices.

We thankfully acknowledge the help we obtained from the MPIK accelerator crew in preparing this work. We gratefully obtained financial support from all research institutions mentioned in the list of affiliations. In addition, the work of KS, AM and SS was partly funded by the

German Research Foundation (DFG) under contract number Mu 1068/20 and within the Priority Programme 1573 under contract number Schi 378/9. ON and DWS were supported in part by the NASA Astronomy and Physics Research and Analysis program and the NASA Solar Heliospheric Physics program.

References

[1] Neu H, Dux R, Kallenbach A, Pütterich T, Balden M , Fuchs J C, Herrmann A , Maggi C F, O'Mullane M, Pugno R, Radivojevic I, Rohde V, Sips A C C, Suttrop W, Whiteford A and the ASDEX Upgrade team 2005 *Nucl. Fusion* **45** 209 – 218
[2] Neu R, Bobkov V, Dux R, Fuchs J C, Gruber O, Herrmann A, Kallenbach A, Maier H, Mayer M, Pütterich T, Rohde V, Sips A C C, Stober J, Sugiyama K and the ASDEX Upgrade Team 2009 *Phys. Scr.* **T138** 014038
[3] ITER Physics Basis Editors 1999 *Nucl. Fusion* **39** 2137
[4] Matthews G F, Edwards P, Hirai T, Kear M, Lioure A, Lomas P, Loving A, Lungu C, Maier H, Mertens P, Neilson D, Neu R, Pamela J, Philipps V, Piazza G, Riccardo V, Rubel M, Ruset C, Villedieu E and Way M 2007 *Phys. Scr.* **T128** 137 – 143
[5] Pütterich T, Neu R, Dux R, Whiteford A D, O'Mullane M G, Summers H P and the ASDEX Upgrade Team 2010 *Nucl. Fusion* **50** 025012
[6] Pütterich T, Neu R, Dux R, Whiteford A D, O'Mullane M G and the ASDEX Upgrade Team 2008 *Plasma Phys. Control. Fusion* **50** 085016
[7] Behar E, Mandelbaum P and Schwob J L 1999 *Phys. Rev. A* **59** 2787
[8] Safronova U I and Safronova A S 2009 *Can. J. Phys.* **87** 83
[9] Peleg A, Behar E, Mandelbaum P and Schwob J L 1998 *Phys. Rev. A* **57** 3493
[10] Ballance C P, Loch S D, Griffin D C and Pindzola M S 2010 *J. Phys. B* **43** 205201
[11] Liesen D 1987 *Phys. Scr.* **36** 723 – 729
[12] Kieslich S, Schippers S, Shi W, Gwinner G, Schnell M, Wolf A, Lindroth E, Tokman M and Müller A 2004 *Phys. Rev. A* **70** 042714
[13] Grieser M, Habs D, von Hahn R, Repnow R, Stampfer M, Jaeschke E, Steck M 1991 *IEEE Part. Acc. Conf.* 2817 – 2819
[14] Schippers S, Bernhardt D, Krantz C, Grieser M, Repnow R, Wolf A, Lestinsky M, Hahn M, Novotný O, Savin D W and Müller A 2011 *Phys. Rev. A* **83** 012711
[15] Cowan R D 1981 *The Theory of Atomic Structure and Spectra* (Berkeley: University of California Press)
[16] Badnell N R, Ballance C P, Griffin D C, O'Mullane M 2012 *Phys. Rev. A* **85** 052716
[17] Rinn K, Müller A, Eichenauer H, Salzborn E 1982 *Rev. Sci. Instrum.* **53** 829
[18] Pedersen H B, Buhr H, Altevogt S, Andrianarijaona V, Kreckel H, Lammich L, de Ruette N, Staicu-Casagrande E M, Schwalm D, Strasser D, Urbain X, Zajfman D and Wolf A 2005 *Phys. Rev. A* **72** 012712
[19] Novotný O, Badnell N R, Bernhardt D, Grieser M, Hahn M, Krantz C, Lestinsky M, Müller A, Repnow R, Schippers S, Wolf A and Savin D W 2012 *Astrophys. J.* **753** 57 1
[20] Hoffknecht A, Uwira O, Schennach S, Frank A,Haselbauer J, Spies W, Angert N, Mokler P H, Becker R, Kleinod M, Schippers S and Müller A 1999 *Phys. Scr.* **T80** 316 – 317
[21] Uwira O, Müller A , Linkemann J, Bartsch T, Brandau C, Schmitt M, Wolf A, Schwalm D, Schuch R, Zong W, Lebius H, Graham W G, Doerfert J and Savin D W 1997 *Hyperfine Interact.* **108** 149 – 154
[22] Lindroth E, Danared H, Glans P, Pešic Z, Tokman M, Vikor G and Schuch R 2001 *Phys. Rev. Lett.* **86** 5027 – 5030
[23] Spruck K et al., in preparation
[24] Spruck K, Badnell N R, Krantz C, Becker A, Bernhardt D, Grieser M, Hahn M, Novotný O, Repnow R, Savin D W, Wolf A, Müller A and Schippers S *J. Phys.: Conf. Ser.* this issue
[25] Dzuba V A, Flambaum V V, Gribakin G F and Harabati C 2012 *Phys. Rev. A* **86** 022714
[26] Flambaum V V, Gribakina A A, Gribakin G F and Harabati C 2002 *Phys. Rev. A* **66** 012713